







## Article

# Optimization of Caper Drying Using Response Surface Methodology and Artificial Neural Networks for Energy Efficiency Characteristics

Hasan Demir <sup>1</sup>, Hande Demir <sup>2</sup>, Biljana Lončar <sup>3</sup>, Lato Pezo <sup>4</sup>, Ivan Brandić <sup>5</sup>, Neven Voća <sup>5,\*</sup>  
and Fatma Yilmaz <sup>6</sup>

<sup>1</sup> Department of Chemical Engineering, Osmaniye Korkut Ata University, 80000 Osmaniye, Türkiye

<sup>2</sup> Department of Food Engineering, Osmaniye Korkut Ata University, 80000 Osmaniye, Türkiye

<sup>3</sup> Faculty of Technology Novi Sad, University of Novi Sad, Bul. Cara Lazara 1, 21000 Novi Sad, Serbia

<sup>4</sup> Institute of General and Physical Chemistry, University of Belgrade, Studentski Trg 12-16, 11000 Belgrade, Serbia

<sup>5</sup> Faculty of Agriculture, University of Zagreb, Svetosimunska cesta 25, 10000 Zagreb, Croatia

<sup>6</sup> Graduate School of Natural and Applied Sciences, Osmaniye Korkut Ata University, 80000 Osmaniye, Türkiye

\* Correspondence: nvoca@agr.hr

**Abstract:** One of the essential factors for the selection of the drying process is energy consumption. This study intended to optimize the drying treatment of capers using convection (CD), refractive window (RWD), and vacuum drying (VD) combined with ultrasonic pretreatment by a comparative approach among artificial neural networks (ANN) and response surface methodology (RSM) focusing on the specific energy consumption (SEC). For this purpose, the effects of drying temperature (50, 60, 70 °C), ultrasonication time (0, 20, 40 min), and drying method (RWD, CD, VD) on the SEC value (MJ/g) were tested using a face-centered central composite design (FCCD). RSM ( $R^2$ : 0.938) determined the optimum drying-temperature-ultrasonication-time values that minimize SEC as; 50 °C-35.5 min, 70 °C-40 min and 70 °C-24 min for RWD, CD and VD, respectively. The conduct of the ANN model is evidenced by the correlation coefficient for training (0.976), testing (0.971) and validation (0.972), which shows the high suitability of the model for optimising specific energy consumption (SEC).

**Keywords:** drying of capers; response surface method; vacuum drying; specific energy consumption; artificial neural network; refractive window drying



**Citation:** Demir, H.; Demir, H.; Lončar, B.; Pezo, L.; Brandić, I.; Voća, N.; Yilmaz, F. Optimization of Caper Drying Using Response Surface Methodology and Artificial Neural Networks for Energy Efficiency Characteristics. *Energies* **2023**, *16*, 1687. <https://doi.org/10.3390/en16041687>

Academic Editor: Antonio

Cano-Ortega

Received: 22 December 2022

Revised: 3 January 2023

Accepted: 6 February 2023

Published: 8 February 2023



**Copyright:** © 2023 by the authors. Licensee MDPI, Basel, Switzerland. This article is an open access article distributed under the terms and conditions of the Creative Commons Attribution (CC BY) license (<https://creativecommons.org/licenses/by/4.0/>).

## 1. Introduction

The caper (*Capparis spinosa* L.), a perennial shrub with thorns, is a member of the Capparis genus. A fragrant and healing plant known as the caper is grown all over the world, but it is most popular in the Mediterranean regions [1]. Caper production numbers are scarce, although the average annual output was estimated to be between 15,000 and 20,000 tons globally [2], with 35% coming mainly from Turkey. The USA, EU, and UK are the three biggest customers in the Capparis trade, which has an annual growth rate of 6% [3]. Drying is one of the crucial preservation techniques to improve long-term storage of food. The storage stability, relatively minimal packing requirements, and lower bulk required for transit are all benefits of dried foods [4]. According to reports, transportation costs significantly affect a country's ability to compete in the global food market [5]. When capers are dried, their storage density is predicted to be lower than when they are canned, resulting in lower shipping costs [4].

The selection of the drying technique is majorly affected by energy usage and the attributes of the dried foods such as fruits, vegetables, and spices in the industry [4,6]. Recently, dryer systems which are supported by renewable energy resources were also

introduced to the food drying process regarding energy saving characteristics [7,8]. Therefore, the selection of the most suitable drying technique may also serve to produce dried food with less structural damage and quality deterioration. Applying pre-treatments before drying is a recent strategy to reduce energy use. However, some of its drawbacks include extended drying times, high temperatures, increased shrinkage, decreased final product quality, and high energy usage [9]. Gilandeh et al. [9] studied the conduct of microwave and convective dryer techniques with ultrasound pre-treatment on specific energy consumption (SEC). Ghasemi and Chayjan, [10] researched the effects of moisture content, particle size, dryer intake air temperature, and dryer infrared power on specific energy consumption parameters of pellets made from food and agricultural wastes. The results showed that finer grinding of raw materials enhanced the specific energy consumption in infrared-convection drying of pellets. The drying of white mulberry fruit by infrared convection was investigated and optimized by RSM and ANN methods regarding to minimization of SEC. The optimum values of SEC were 166.6 MJ/kg with a desirability of 0.9670. According to the statistical indices, the feed and cascade-forward back-propagation neural systems with the Levenberg–Marquardt training method and topologies of 3-10-1 were the best neural models to forecast SEC [11]. Jarahizadeh and Dinani, [12] investigated the effect of sonication time and sonication power on the execution of drying potato slices by RSM regarding the energy savings in the drying process. In comparison of ultrasound pretreatments and pure convective drying, the application of ultrasound pretreatments decreased the processing time, and SEC values of drying process of potato slices.

The improving food preservation methods for long-term storage has been one of the main concerns of the industry. The principal aim of the industry was drying vegetables and fruits to create dehydrated goods with excellent quality and a long-term storage with lowest energy usage. According to our best knowledge, dehydration of capers addressing the optimization of caper drying utilizing RSM and ANN approach in the manner of Energy Efficiency has not been reported yet. Therefore, the scope of this study was to study the impact of drying temperature (50, 60, 70 °C), ultrasonication duration (0, 20, 40 min), and drying technique (RWD, CD, VD) on the SEC value (MJ/g) applying an experimental design, response surface approach, and artificial neural networks. Using analysis of variance, a Face-Centered Central Composite Design (FCCD) with 39 runs was used to build the model (ANOVA). The threshold for significance was set at 0.05. Response values, which represented the quantity of electrical energy used, were calculated according to the magnitude of energy used by the ultrasonic drying bath, ventilation fan, vacuum pump, and electric heater. The optimum points were determined according to the maximum desirability factor. The effects of factors on SEC values were analyzed by ANOVA table, response surface plots, normality plot of residuals, and ANN.

## 2. Materials and Methods

### 2.1. Drying Methods and Procedure

The capers were purchased in a brine solution in a glass container from the store. For conventional drying method, a laboratory type oven (JSR, JSON—250) was applied for dehydration until the defined weight base percentage was reached (89.5%). The weight of capers was measured with digital analytical balance (Radwag, AS/X, Radom, Poland) in a range of 0–200 g. The experimental temperatures were 50, 60, and 70 °C. In all drying operations, the air velocity was at 0.5 m s<sup>-1</sup>.

Vacuum drying was achieved by a vacuum oven (Vacucell–111 standard, München, Germany) with a rotary vane vacuum pump (Zhejiang Sujing, Wx–2 model, Shaoxing, China), having 2 L/s speed of pump and 1400 r/min revolution speed. The vacuum pump was used for reducing the pressure to 0.1 bar level inside the vacuum oven. The experimental temperatures were 50, 60, and 70 °C. The caper sample was placed in stainless steel sieve basket after the adjusted temperature was attained. The vacuum pump was started, and dehydration began. The velocity of air in the oven was 1.5 m s<sup>-1</sup>. The

dehydration in the vacuum oven was continued until the defined weight base percentage of (89.5%) was obtained [13].

The refractive window drying (RWD) method was employed for the drying process on capers. Mylar film was laid to cover the 50, 60, and 70 °C water bath and the drying process was carried out for through the defined weight base percentage (89.5%) as presented in Figure 1. Finally, electricity consumption was measured by using digital electric meters for all drying processes.

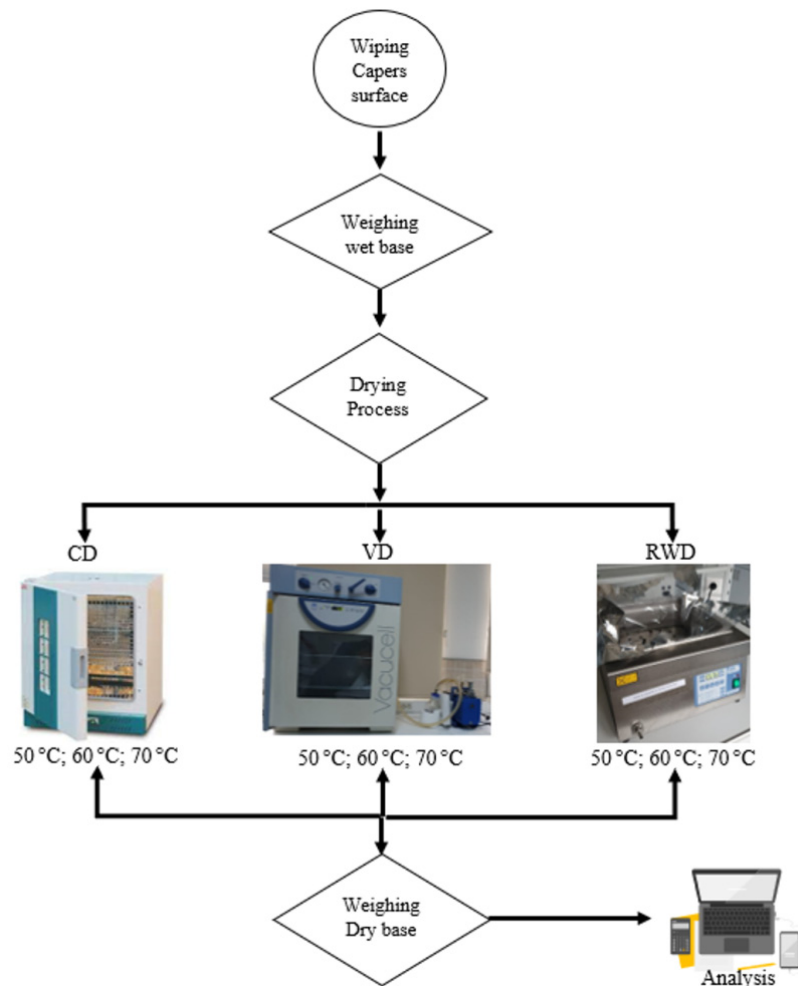


Figure 1. Capers drying process flowsheet.

## 2.2. Specific Energy Consumption

The consumed electrical energy was calculated as the total consumption energy ( $E_T$ ), involving the energy consumption of the electric heater, the ventilator fan, vacuum pump, and the ultrasonic bath according to drying methods. The SEC can be evaluated by dividing  $E_T$  by amount of water evaporated during the drying process as in the following equation [14].

$$SEC = \frac{E_T}{\text{Weight loss of Capers (g)}} \quad (1)$$

The energy consumption values that correspond to the total work of the process carried out under specific circumstances, including the selection of the environmental parameters (moisture, temperature, and particle size composition) that are most appropriate, are characterized by the lowest unit energy consumption as well as a decrease in the emission of pollutants into air [15].

### 2.3. Optimization Methods

Experimental design and RSM approach were utilized to consider the effects of drying temperature ( $X_1$ : 50, 60, 70 °C), ultrasonication time ( $X_2$ : 0, 20, 40 min) and drying method ( $X_3$ : RWD, CD, VD) on the SEC value (MJ/g). A Face-Centered Central Composite Design (FCCD) with 39 runs was employed to construct the model through analysis of variance (ANOVA) applying the trial version of Design Expert v.11.0 software (Stat-Ease, Inc., Minneapolis, MN, USA) [16]. The statistical significance level was taken as  $p \leq 0.05$ . The response values obtained according to the experimental design were fitted to a second-order polynomial model. The model equation given in Equation (2) is applied to estimate the impacts of linear, quadratic, and/or interaction terms of the independent variables on second order polynomial:

$$Y = \beta_0 + \sum_{i=1}^2 \beta_i X_i + \sum_{i=1}^2 \beta_{ii} X_i^2 + \beta_{ij} X_i X_j \quad (2)$$

where  $Y$  was the variable of response,  $X_i$  and  $X_j$  were independent factors,  $\beta_0$  was the intercept, and  $\beta_i$ ,  $\beta_{ii}$ , and  $\beta_{ij}$  were constants for linear, quadratic, and factor interaction terms, respectively.

The classical machine learning models such as artificial neural network (ANN), random forest regression (RFR), support vector machine (SVM), extreme learning machine (ELM), K-nearest neighbors (KNN), and decision tree (DT) are widely used in modelling in various branches of science [17,18]. The SVM is a widely used modelling technique based on the statistical learning theory, well recognized for its strong generalization ability. The optimal network is obtained by exploring the balance among the complexity of the model and the training error [19]. The ELM designs a single-layer feedforward network by randomly generating the input weights and biases of the hidden layers [20].

The vast variety of state-of-the-art machine learning techniques are suitable for sequence data such as ensemble learning models, such as XGBoost [21], LightGBM [22], and CatBoost. The XGBoost model exerts its advantages especially for high prediction accuracy and interpretability. LightGBM model enables large amounts of data and GPU training. The LightGBM models are proven to be more accurate and faster than XGBoost. Data fusion enables stronger forecasting accuracy, according to the integration of gradient boosting based categorical attributes supported by CatBoost algorithm [23].

A multi-layer perceptron (MLP) architecture, having three layers (input, hidden, and output) were utilized for modelling the ANN for the prediction of SEC values and temperature. Multiple researchers have established ANN as a method for drying kinetics prediction, acquiring accurate and elevated precision results concerning fruit and vegetable drying [24–26]. The database was standardized before to ANN computation to increase the ANN model's accuracy.

### 2.4. Statistical Analysis

The laboratory data were statistically evaluated using multivariable mathematical approaches such as Artificial Neural Network modeling, and global sensitivity analysis using StatSoft Statistica, ver. 10.0, Palo Alto, CA, USA. In addition, the diagram was drawn with R software v.4.0.3 (64-bit version) with the “circle” method, upper type.

#### 2.4.1. ANN Modelling

As previously described by Voća et al. [27], using a multi-layer perceptron model (MLP), the ANN model with a high possibility for nonlinear function analysis was created. In order to improve the results of the ANN modeling, before the ANN model calculation, it was necessary to normalize input and output data [28]. The first step of the ANN modelling is the ANN building, which requires frequently inserted input data in the network [29,30]. The training process of the network was conducted as previously reported by Rajković et al. [31]. The weight coefficients and biases associated with the hidden and output layers

were presented in the form of matrices  $W_1$  and  $W_2$  and vectors  $B_1$  and  $B_2$ . The following formula reveals the neural network model:

$$Y = f_1(W_2 \cdot f_2(W_1 \cdot X + B_1) + B_2) \quad (3)$$

where  $Y$  was the outputs matrix,  $f_1$  and  $f_2$  were the hidden and output layers transfer functions, accordingly, and  $X$  was the matrix of inputs [32].

Throughout the training cycle, the weight coefficients  $W_1$  and  $W_2$  were determined while continually adding the components, using an optimization strategy to reduce the variance between the experimental data and the created model [33]. The ANN model was created to anticipate and optimize the specific energy consumption, according to temperature, time, and drying treatment (CD, RWD, and VD).

#### 2.4.2. Global Sensitivity Analysis

In order to investigate the relative importance of the input parameters (T, t, CV, VD, and RWD) on the output variable (SEC), relying on the obtained ANN model weight coefficients, Yoon's global sensitivity equation was used [34]:

$$RI_{ij}(\%) = \frac{\sum_{k=0}^n (w_{ik} \cdot w_{kj})}{\sum_{i=0}^m \left| \sum_{k=0}^n (w_{ik} \cdot w_{kj}) \right|} \cdot 100\% \quad (4)$$

where:  $i$ —input variable,  $j$ —output variable,  $k$ —hidden neuron,  $w$ —weight coefficient in ANN model,  $n$ —number of hidden neurons,  $m$ —number of inputs.

#### 2.4.3. Error Analysis

The created ANN model was validated by the coefficient of determination ( $R^2$ ), reduced chi-square ( $\chi^2$ ), root mean square error (RMSE), mean bias error (MBE), and mean percentage error (MPE), applying the following equations [35]:

$$\chi^2 = \frac{\sum_{i=1}^N (x_{\text{exp},i} - x_{\text{pre},i})^2}{N - n} \quad (5)$$

$$\text{RMSE} = \left[ \frac{1}{N} \cdot \sum_{i=1}^N (x_{\text{pre},i} - x_{\text{exp},i})^2 \right]^{1/2} \quad (6)$$

$$\text{MBE} = \frac{1}{N} \cdot \sum_{i=1}^N (x_{\text{pre},i} - x_{\text{exp},i}) \quad (7)$$

$$\text{MPE} = \frac{100}{N} \cdot \sum_{i=1}^N \left( \frac{|x_{\text{pre},i} - x_{\text{exp},i}|}{x_{\text{exp},i}} \right) \quad (8)$$

where  $x_{\text{pre},i}$  present value obtained by the model, and  $x_{\text{exp},i}$  marks the experimental values  $n$  and  $N$  were the number of constants and observations, respectively.

### 3. Results and Discussion

#### 3.1. Optimization of Drying Conditions to Minimize SEC by RSM

In order to choose the most cost-effective drying method, energy consumption must be taken into account. According to this study, a face-centered central composite design with 13 runs for each drying method was involved to optimize the processing temperature and ultrasonication time conditions that minimize the specific energy consumption required to dehydrate capers from an initial MC to final MC (about 10% dry basis). The SEC values obtained during RWD, CD and VD of capers were given in Table 1. According to Table 1, SEC for RWD, CD and VD ranged between 3.8–7.8 MJ/g, 1.4–3.3 MJ/g and 4.6–13.7 MJ/g, respectively. RSM was utilized to construct the models that reflect the impact of indepen-

dent variables on the SEC response. According to ANOVA results (Table 2), the factors with significant ( $p \leq 0.05$ ) main effect on SEC were drying temperature, ultrasonication time, and drying method. However, the interaction between drying temperature and drying method was also found to have a significant ( $p \leq 0.05$ ) effect on SEC. Although there was no statistically significant ( $p \leq 0.05$ ) interaction between drying temperature and ultrasonication time, pretreatment of capers with ultrasonication led to structural damage on plant structure [36], increased water removal from capers, and a shorter drying time. A competitive  $R^2$  value (0.938) indicates the empirical models can be applied to foresee the SEC values with 93.82% convenience. Less than 20% difference between predicted  $R^2$  and adjusted  $R^2$  values means that the model was the best fit for selected responses, which was valid for our model (Table 2).

**Table 1.** Face-centered central composite design of factors with experimental SEC values.

Run No	Independent Variables			Response Variable
	Drying Temperature (°C) ( $X_1$ )	Ultrasonication Time (min) ( $X_2$ )	Drying Method ( $X_3$ )	SEC (MJ/g)
1	60	20	RWD	5.2
2	60	20	VD	5.9
3	60	40	CD	1.7
4	60	20	RWD	5.4
5	70	20	RWD	6.1
6	60	0	RWD	7.8
7	70	40	CD	1.4
8	60	20	RWD	3.8
9	60	0	VD	8.4
10	50	0	VD	13.7
11	50	20	VD	8.8
12	50	20	CD	2.0
13	60	20	CD	2.3
14	50	0	CD	3.3
15	60	20	RWD	5.6
16	70	40	RWD	4.5
17	70	0	RWD	6.2
18	50	40	VD	8.6
19	60	20	VD	6.4
20	50	40	CD	1.6
21	60	40	VD	4.6
22	60	20	VD	6.4
23	50	0	RWD	6.7
24	60	20	VD	8.7
25	70	40	VD	6.0
26	70	0	CD	3.3
27	60	20	CD	2.7
28	50	20	RWD	4.3
29	50	40	RWD	5.0
30	60	40	RWD	4.7
31	60	20	VD	6.9
32	60	0	CD	3.2
33	70	20	CD	1.8
34	60	20	CD	2.5
35	60	20	RWD	6.3
36	70	0	VD	6.2
37	70	20	VD	4.6
38	60	20	CD	2.7
39	60	20	CD	2.7

RWD: Refractive Window Drying, CD: Convective Drying, VD: Vacuum Drying, SEC: Specific Energy Consumption.

**Table 2.** Analysis of variance (ANOVA) for the fitted design model for optimization of drying conditions.

Source	SS	DF	MS	F	p
Model	234.7	17	13.8	18.8	<0.001
$X_1$ —drying temperature	10.7	1	10.7	14.6	0.001
$X_2$ —ultrasonication time	23.8	1	23.8	32.3	<0.001
$X_3$ —drying method	161.2	2	80.6	109.5	<0.001
$X_1 \times X_2$	1.8	1	1.8	2.5	0.129
$X_1 \times X_3$	23.5	2	11.7	16.0	<0.001
$X_2 \times X_3$	1.4	2	0.7	0.9	0.409
$X_1^2$	0.0	1	0.0	0.1	0.806
$X_2^2$	2.4	1	2.4	3.3	0.084
$X_1 \times X_2 \times X_3$	4.2	2	2.1	2.8	0.081
$X_1^2 \times X_3$	3.1	2	1.6	2.1	0.144
$X_2^2 \times X_3$	0.6	2	0.3	0.4	0.689
Residual	15.5	21	0.7		
Lack of Fit	7.3	9	0.8	1.2	0.388
Pure Error	8.2	12	0.7		
Cor Total	250.2	38			

$$R^2 = 0.938, \text{ Adjusted } R^2 = 0.888, \text{ Predicted } R^2 = 0.713$$

DF: degrees of freedom, SS: sum of squares, MS: mean squares.

The second-order polynomial regression equations obtained for SEC relating to actual levels of drying conditions for RWD, CD, and VD were given in Equations (9)–(11). In Equation (9), the drying temperature has an increasing effect, whereas ultrasonication time has a decreasing effect on the SEC of RWD. A similar trend was valid for the CD of capers (Equation (10)). On the contrary, drying temperature has a decreasing effect on the SEC of the VD method (Equation (11)), which means a higher level of drying temperature causes lower SEC values, especially with higher ultrasonication time.

$$SEC_{RWD} = -6.08 + 0.43 \times X_1 - 0.12 \times X_2 + 3.2 \times 10^{-17} \times X_1 \times X_2 - 0.003 \times X_1^2 + 0.002 \times X_2^2 \quad (9)$$

$$SEC_{CD} = -9.91 + 0.45 \times X_1 - 0.04 \times X_2 - 3.2 \times 10^{-17} \times X_1 \times X_2 - 0.004 \times X_1^2 + 0.001 \times X_2^2 \quad (10)$$

$$SEC_{VD} = 64.41 - 1.49 \times X_1 - 0.52 \times X_2 + 0.01 \times 10^{-17} \times X_1 \times X_2 + 0.001 \times X_1^2 + 0.002 \times X_2^2 \quad (11)$$

The response surface plots of the three constructed models on SEC are given in Figure 2a–c. Even though the ultrasonication process and drying at relatively higher temperatures has a role in the consumption of energy, the SEC value decreased as the ultrasonication time increased from 0 to 40 min and the drying temperature increased from 50 to 70 °C for all three drying methods (Figure 2a–c).

The decrease in SEC was a consequence of the ultrasonication pretreatment that successfully reduced the time required to dry the capers [37]. Similar findings for SEC values were made by Motevali et al. [38], who showed that the increment in drying temperature exhibits a declining trend for SEC values. Similarly, the SEC values have decreased as a result of the shorter drying time brought on by rising temperatures [39]. The comparison of SEC values among the three investigated drying methods demonstrated that, at the center point of ultrasonication time, the most cost-effective drying method was CD, as can be observed in Figure 2d.

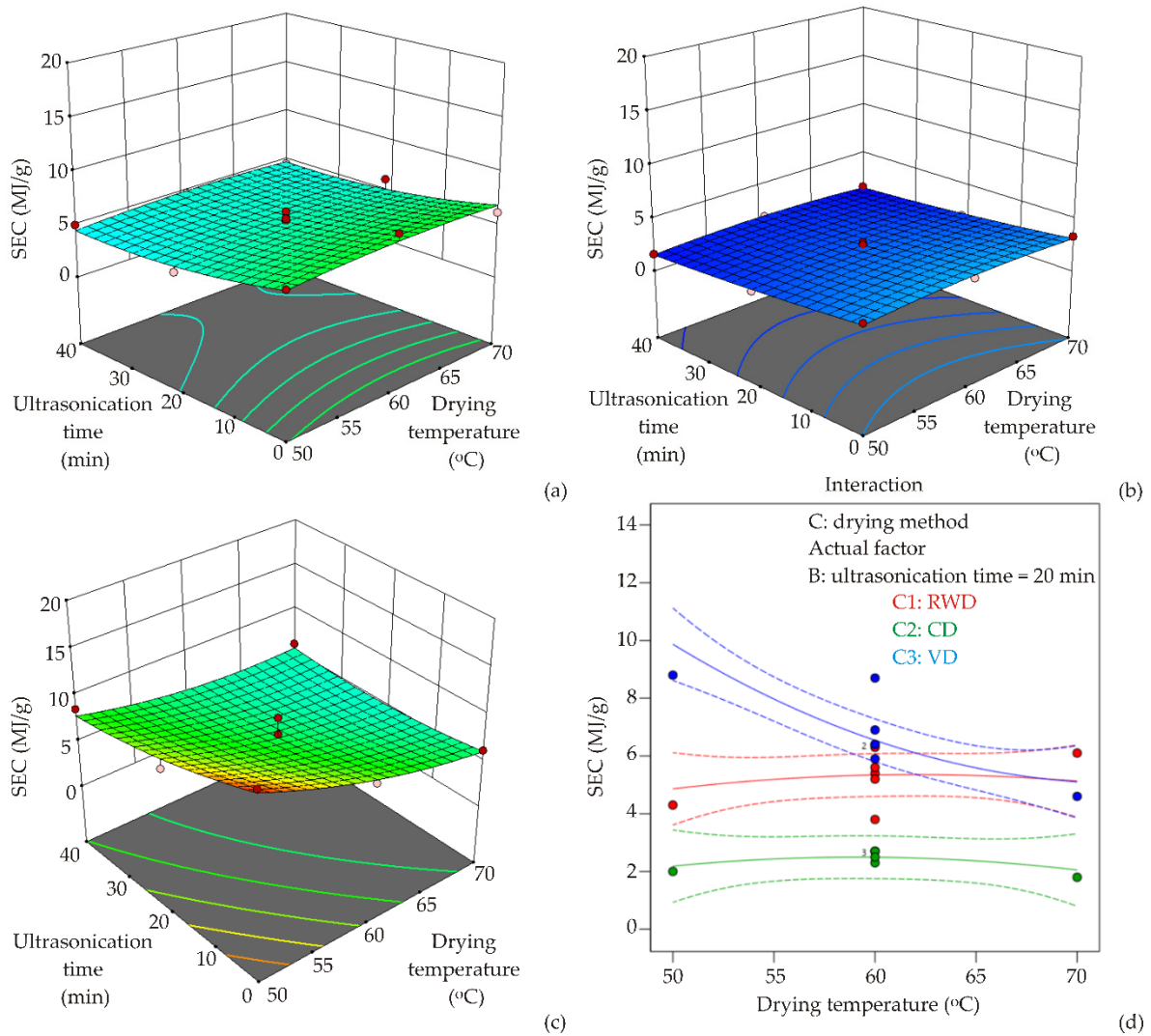


**Figure 2.** Response surface plots for  $X_1$ – $X_2$  interaction of (a) RWD, (b) CD, (c) VD and (d) line plot for  $X_1$ – $X_3$  interaction on SEC.

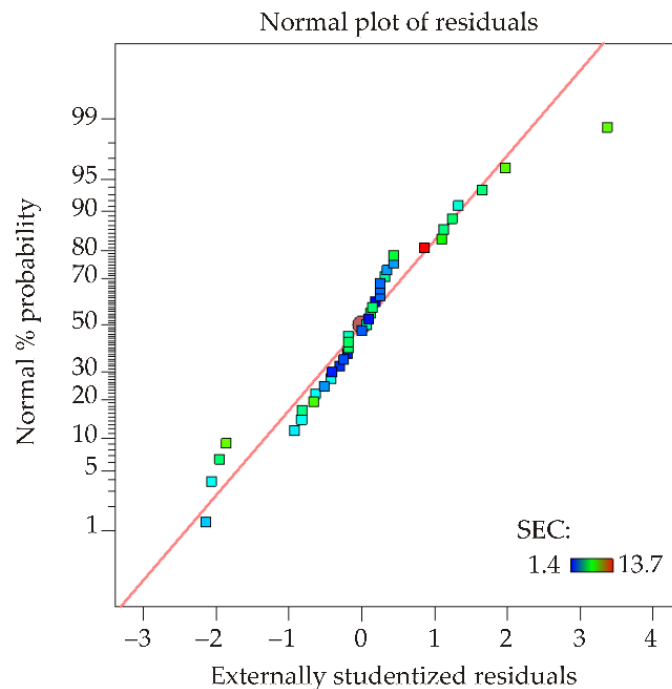
The optimum drying-temperature–ultrasonication-time values for RWD, CD, and VD were 50 °C–35.5 min, 70 °C–40 min, and 70 °C–24 min, respectively. The optimum points were determined according to the maximum desirability factor. The desirability values for RWD, CD, and VD drying methods were 0.752, 1.0, and 0.701, respectively. The optimum conditions from each drying method were examined once more to confirm the predictive capability of the built models. Experimental results and SEC values predicted by Equations (9)–(11) were given in Table 3. Error percentages must be as low as possible. As can be seen in Table 3, all error percentages were less than 8% and the most accurate model belonged to RWD with the least error percentage. The normal plot of residuals (Figure 3) shows normally distributed residuals that were in a symmetrical pattern with a constant spread centered on zero [40]. The limit of error for each response was within a tolerable range as shown in Table 3, which supports the correctness of the established response models. The model’s viability and consistency were demonstrated by the relative errors of modeled and experimental values being less than 10% (Table 3) [41–43].



**Table 3.** ANN model summary (performance and errors).

Network Name	Performance			Error			Training Algorithm	Error Function	Hidden Activation	Output Activation
	Train.	Test.	Valid.	Train.	Test.	Valid.				
MLP 5-10-1	0.976	0.971	0.972	0.116	0.709	0.359	BFGS 42	SOS	Exponential	Identity

Performance term describes the coefficients of determination, while error terms show the ANN model lack of data.

**Figure 3.** Normality plot of residuals obtained by RSM.

### 3.2. ANN Model

The influence of drying temperature, processing time, and drying type (RWD, CD, and VD) on the SEC was researched with the ANN model. The ideal neural network constructed displayed high generalization capabilities for the testing data and could properly predict the output parameters of the drying samples given the observed input parameters. Based on ANN developed, the optimal number of the hidden layer neurons for the SEC was 10 (network MLP 5-10-1), focusing on achieving the high coefficient of determination.  $R^2$  (overall 0.976 for ANN throughout the training period) and lower values of SOS (Table 3).

The performance of ANN described with coefficients of determination ( $R^2$ ) between experimentally measured and ANN outputs during training, testing and validation steps as shown in Table 4.

**Table 4.** Coefficients of determination ( $R^2$ ) during training, testing and validation steps.

	Train	Test	Validation
1.MLP 5-3-1	0.976	0.971	0.972

The obtained weights and biases obtained during ANN modeling were shown in Tables 5 and 6, calculated according to Equation (3).

ANN model was exploited to foresee an experimental set of values, quite adequately, for the selected parameters as shown in Figure 4 where the experimental and ANN model data were presented.

**Table 5.** The weight coefficients and biases  $W_1$  and  $B_1$ .

	1	2	3	4	5	6	7	8	9	10
T	−3.381	−0.627	−1.471	−3.081	0.330	−0.465	−1.424	−0.671	0.143	−1.357
t	1.760	−0.577	−1.341	0.312	0.296	0.300	0.158	0.422	−0.206	1.462
CD	−0.575	0.087	−0.778	0.057	−0.834	−0.335	−0.296	0.098	−0.271	−0.232
VD	0.490	0.392	−0.381	0.815	0.356	0.400	−0.510	0.009	−0.312	0.188
RWD	−0.039	−0.328	1.113	−1.218	0.559	−0.089	0.420	−0.255	0.539	−0.094
bias	0.007	0.107	0.056	−0.292	0.103	0.097	−0.306	−0.087	0.006	−0.131

**Table 6.** The weight coefficients and biases  $W_2$  and  $B_2$ .

	1	2	3	4	5	6	7	8	9	10	Bias
SEC	0.161	0.746	0.468	−0.457	0.335	−0.254	−0.135	0.316	−0.197	−0.148	−0.383

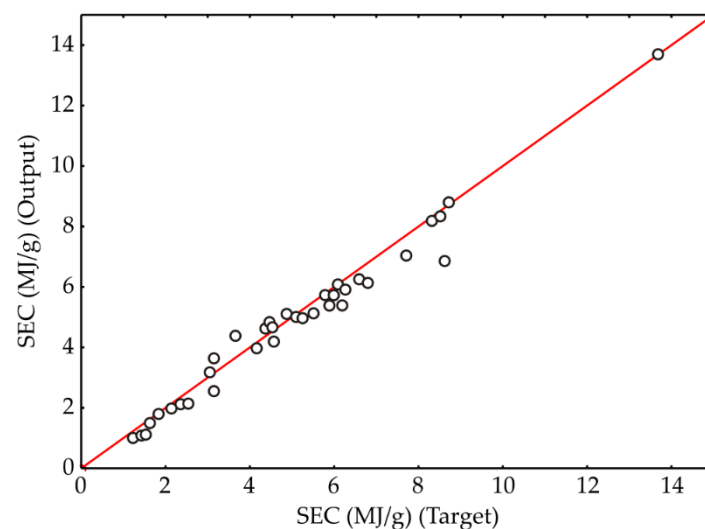
**Figure 4.** Comparison among experimentally gained and ANN model delivered values of SEC.

Figure 4 presents the experimental and ANN model predicted data, revealing that the ANN model adequately predicted observed variable. Additionally, the SOS performed by the ANN model was of the same size as the experimental errors. In contrast, the predicted values were like the preferred values concerning the ANN model  $R^2$  value.

### 3.2.1. The Exactness of the Models

The obtained model results were verified as follows: the  $R^2$ ,  $\chi^2$ , MBE, RMSE, and MPE were calculated, Table 7. The results reveal that the ANN model had an insignificant lack of fit tests, which indicates that the model adequately anticipated the values of the analyzed parameters.

**Table 7.** Goodness of fit parameters.

Model	$\chi^2$	RMSE	MBE	MPE	$R^2$
ANN	0.457	0.668	−0.064	10.408	0.932
RWD	0.501	0.680	0.000	10.430	0.587
CD	0.036	0.183	0.000	6.862	0.916
VD	0.751	0.833	0.000	9.088	0.870

### 3.2.2. Optimization of Drying Conditions to Minimize SEC by ANN

The results of ANN optimization were achieved by analyzing the model described in Equation (1). The primary goal of this research was to minimize the SEC value using SOP and ANN models while changing drying temperature, ultrasonication time or drying method. The domain of the experimental variable was utilized to define the required parameter range for the optimization. The maximum calculated values for SEC were 70 °C, 40 min, and CD drying method, respectively (Table 8).

**Table 8.** Predicted and experimental values of SEC for RSM and ANN models validation.

Run No	Drying Temperature (°C)	Ultrasonication Time (min)	Drying Method	Actual SEC (MJ/g)	RSM Predicted SEC (MJ/g)	RSM Error (%)	ANN Predicted SEC (MJ/g)	ANN Error (%)
1	50	35.5	RWD	4.60	4.45	3.26	4.68	1.74
2	70	40	CD	1.45	1.34	7.59	1.52	2.07
3	70	24	VD	4.90	5.08	3.67	4.93	0.61

### 3.2.3. Global Sensitivity Analysis—Yoon’s Interpretation Method

Yoon’s global sensitivity equation, which corresponds to the weight coefficients of the generated ANN model, was used to examine the impacts of drying circumstances and drying type parameters (temperature and time) on the SEC [44]. Following the ANN global sensitivity analysis, the graphical illustration of Yoon’s interpretation method results was presented in Figure 5. Based on Figure 5, all observer parameters positively influenced the SEC. The processing time was a more influential parameter positively influencing SEC than drying temperature, with an approximately relative influence of 17.88%. On the other hand, the VD was the most positively influential parameter on the SEC with the relative importance of 46.89%. The positive influence on the SEC was also observed for CD (28.23%) and RWD (9.66%), Figure 5.

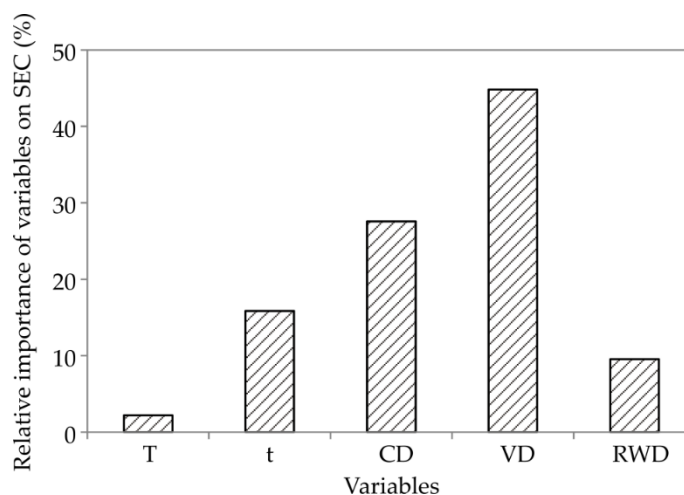


**Figure 5.** The relative importance of T, t, CD, VD and RWD on SEC.

## 4. Conclusions

The energy consumption values that correspond to the total work of the process carried out under specific circumstances, including the selection of the environmental parameters (moisture, temperature, and particle size composition) that are most appropriate, are characterized by the lowest unit energy consumption as well as a decrease in the emission of pollutants into air.

This study has focused on the optimization of the caper drying process, emphasizing the determination of the most energy-efficient drying method combined with ultrasonication pretreatment. The drying conditions for RWD, CD, and VD were expressed as

Second-order polynomial regression equations obtained for SEC. For RWD and CD, drying temperature was found to have an increasing and ultrasonication time decreasing effect on SEC. However, a different behavior was obtained for the VD method as, a higher drying temperature level lowered the SEC values specific to higher ultrasonication time levels. The optimum drying-temperature-ultrasonication-time conditions that minimize specific energy consumption for three drying methods were successfully predicted by RSM as; 50 °C-35.5 min (4.45 MJ/g), 70 °C-40 min (1.34 MJ/g) and 70 °C-24 min (5.08 MJ/g) for RWD, CD, and VD, respectively. It was evident that ultrasonication pretreatment had a major role in the reduction of SEC value even at relatively higher drying temperatures for all three drying methods. This study revealed that RSM could provide a basis for adequate precision in the possible practical use of the energy-efficient caper drying. Validation of the models for SEC optimization showed that the ANN had a lower overall error. In three validation cycles, the RSM model showed a slightly higher error (3.26%, 7.59%, and 3.67%), while the ANN model predicted a lower error (1.74%, 2.07%, and 0.61%). Although both models were effective, the ANN model was a more reliable tool for optimizing SEC.

**Author Contributions:** Conceptualization, H.D. (Hasan Demir), H.D. (Hande Demir) and B.L.; methodology, H.D. (Hande Demir) and F.Y.; software, L.P., I.B. and B.L.; validation, H.D. (Hande Demir); formal analysis, H.D. (Hasan Demir), H.D. (Hande Demir) and B.L.; investigation, H.D. (Hande Demir); resources, H.D. (Hasan Demir) and H.D. (Hande Demir); data curation, H.D. (Hasan Demir), H.D. (Hande Demir) and B.L.; writing—original draft preparation, H.D. (Hasan Demir), H.D. (Hande Demir) and B.L.; writing—review and editing, N.V. and L.P.; project administration, H.D. (Hasan Demir); funding acquisition, H.D. (Hasan Demir) and N.V. All authors have read and agreed to the published version of the manuscript.

**Funding:** This research was funded by OKÜBAP (Scientific Research Projects Unit of Osmaniye Korkut Ata University) with the project number OKÜBAP-2021-PT3-016. and by the Ministry of Science Technological Development and Innovations of the Republic of Serbia, grant numbers 451-03-68/2022-14/200134 and 451-03-68/2022-14/200051.

**Data Availability Statement:** All data generated or analyzed during this study are included in this published article.

**Conflicts of Interest:** The authors declare no conflict of interest.

## References

1. Shahrajabian, M.H.; Sun, W.; Cheng, Q. Plant of the Millennium, Caper (*Capparis spinosa* L.), chemical composition and medicinal uses. *Bull. Natl. Res. Cent.* **2021**, *45*, 131. [[CrossRef](#)]
2. Ikromjonovich, A.Z.; Turgunovich, M.A. Factors affecting quality in the production of organic products from buds and fruits of capers (*Capparis spinosa*). *Int. J. Sci. Res.* **2022**, *3*, 311–319.
3. Reyahi-Khoram, M.; Reyahi-Khoram, R. Early Feasibility Study on Capparis Production and Processing in Hamedan Province in Iran. *J. Adv. Agric. Technol.* **2018**, *5*, 313–317. [[CrossRef](#)]
4. Hnin, K.K.; Zhang, M.; Mujumdar, A.S.; Zhu, Y. Emerging food drying technologies with energy-saving characteristics: A review. *Dry. Technol.* **2019**, *37*, 1465–1480. [[CrossRef](#)]
5. Wilmsmeier, G.; Sanchez, R.J. The relevance of international transport costs on food prices: Endogenous and exogenous effects. *Res. Transp. Econ.* **2009**, *25*, 56–66. [[CrossRef](#)]
6. Demir, H.; Cihan, E.; Demir, H. 3D simulation of transport phenomena of onion drying with moving boundary in a vacuum oven. *J. Food Process. Eng.* **2020**, *43*, 4. [[CrossRef](#)]
7. Hürdoğan, E.; Çerçi, K.N.; Saydam, B.D.; Özalp, C. Experimental and modeling study of peanut drying in a solar dryer with a novel type of a drying chamber. *Energy Sources Part A Recovery Util. Environ. Eff.* **2022**, *44*, 5586–5609. [[CrossRef](#)]
8. Çerçi, K.N.; Hürdoğan, E. Performance assessment of a heat pump assisted rotary desiccant dryer for low temperature peanut drying. *Biosyst. Eng.* **2022**, *223*, 1–17. [[CrossRef](#)]
9. Gilandeh, Y.A.; Kaveh, M.; Jahanbakhshi, A. The effect of microwave and convective dryer with ultrasound pre-treatment on drying and quality properties of walnut Kernel. *J. Food Process. Preserv.* **2019**, *43*, e14178. [[CrossRef](#)]
10. Ghasemi, A.; Chayjan, R.A. Optimization of Pelleting and Infrared-Convection Drying Processes of Food and Agricultural Waste Using Response Surface Methodology (RSM). *Waste Biomass Valorization* **2019**, *10*, 1711–1729. [[CrossRef](#)]
11. Golpour, I.; Kaveh, M.; Chayjan, R.A.; Guiné, R.P.F. Optimization of Infrared-convective Drying of White Mulberry Fruit Using Response Surface Methodology and Development of a Predictive Model through Artificial Neural Network. *Int. J. Fruit Sci.* **2020**, *20*, S1015–S1035. [[CrossRef](#)]

12. Jarahizadeh, H.; Dinani, S.T. Influence of applied time and power of ultrasonic pretreatment on convective drying of potato slices. *Food Sci. Biotechnol.* **2019**, *28*, 365–376. [[CrossRef](#)]
13. Süfer, Ö.; Sezer, S.; Demir, H. Thin layer mathematical modeling of convective, vacuum and microwave drying of intact and brined onion slices. *J. Food Process. Preserv.* **2017**, *41*, e13239. [[CrossRef](#)]
14. EL-Mesery, H.S.; Abomohra, A.E.; Kang, C.U.; Cheon, J.K.; Basak, B.; Jeon, B.H. Evaluation of Infrared Radiation Combined with Hot Air Convection for Energy-Efficient Drying of Biomass. *Energies* **2019**, *12*, 2818. [[CrossRef](#)]
15. Roman, K.; Barwicki, J.; Rządziejewicz, W.; Dawidowski, M. Evaluation of Mechanical and Energetic Properties of the Forest Residues Shredded Chips during Briquetting Process. *Energies* **2021**, *14*, 3270. [[CrossRef](#)]
16. Demir, H.; Sezer, S.; Süfer, Ö. Soğan dilimlerinin kurutulması esnasında renk değişimine etki eden faktörlerin yanıt yüzey yöntemi ile belirlenmesi. *GIDA* **2017**, *42*, 731–742. [[CrossRef](#)]
17. Sajjad, U.; Hussain, I.; Raza, W.; Sultan, M.; Alarifi, I.M.; Wang, C.-C. On the Critical Heat Flux Assessment of Micro- and Nanoscale Roughened Surfaces. *Nanomaterials* **2022**, *12*, 3256. [[CrossRef](#)]
18. Rajković, D.; Marjanović Jeromela, A.; Pezo, L.; Lončar, B.; Grahovac, N.; Kondić Špika, A. Artificial neural network and random forest regression models for modelling fatty acid and tocopherol content in oil of winter rapeseed. *J. Food Compos. Anal.* **2023**, *115*, 105020. [[CrossRef](#)]
19. Ma, H.; Ding, F.; Wang, Y. A novel multi-innovation gradient support vector machine regression method. *ISA Trans.* **2022**, *130*, 343–359. [[CrossRef](#)]
20. Wang, C.; Peng, G.; De Baets, B. Embedding metric learning into an extreme learning machine for scene recognition. *Expert Syst. Appl.* **2022**, *203*, 117505. [[CrossRef](#)]
21. Su, J.; Wang, Y.; Niu, X.; Shaa, S.; Yu, J. Prediction of ground surface settlement by shield tunneling using XGBoost and Bayesian Optimization. *Eng. Appl. Artif. Intell.* **2022**, *114*, 105020. [[CrossRef](#)]
22. Jawad, M.; Ghulam-e, M.; Muhammad, A. Accurate estimation of tool wear levels during milling, drilling and turning operations by designing novel hyperparameter tuned models based on LightGBM and stacking. *Measurement* **2022**, *190*, 110722. [[CrossRef](#)]
23. Dutta, J.; Roy, S. OccupancySense: Context-based indoor occupancy detection & prediction using CatBoost model. *Appl. Soft Comput.* **2022**, *119*, 108536. [[CrossRef](#)]
24. Aghbashlo, M.; Hosseinpour, S.; Mujumdar, A.S. Application of artificial neural networks (ANN) in drying technology: A comprehensive review. *Dry. Technol.* **2015**, *33*, 1397–1462. [[CrossRef](#)]
25. Chasiotis, V.K.; Tzempelikos, D.A.; Filios, A.E.; Moustris, K.P. Artificial neural network modelling of moisture content evolution for convective drying of cylindrical quince slices. *Comput. Electron. Agric.* **2020**, *172*, 105074. [[CrossRef](#)]
26. Fabani, M.P.; Capossio, J.P.; Román, M.C.; Zhu, W.; Rodriguez, R.; Mazza, G. Producing non-traditional flour from watermelon rind pomace: Artificial neural network (ANN) modeling of the drying process. *J. Environ. Manag.* **2021**, *281*, 111915. [[CrossRef](#)]
27. Voća, N.; Pezo, L.; Jukić, Ž.; Lončar, B.; Šuput, D.; Krička, T. Estimation of the storage properties of rapeseeds using an artificial neural network. *Ind. Crops Prod.* **2022**, *187*, 115358. [[CrossRef](#)]
28. Vojnov, B.; Jaćimović, G.; Šeremešić, S.; Pezo, L.; Lončar, B.; Krstić, Đ.; Vujić, S.; Čupina, B. The Effects of Winter Cover Crops on Maize Yield and Crop Performance in Semiarid Conditions—Artificial Neural Network Approach. *Agronomy* **2022**, *12*, 2670. [[CrossRef](#)]
29. Šovljanski, O.; Šeregelj, V.; Pezo, L.; Tumbas Šaponjac, V.; Vulić, J.; Cvanić, T.; Markov, S.; Četković, G.; Čanadanović-Brunet, J. Horned Melon Pulp, Peel, and Seed: New Insight into Phytochemical and Biological Properties. *Antioxidants* **2022**, *11*, 825. [[CrossRef](#)]
30. Puntarić, E.; Pezo, L.; Zgorelec, Ž.; Gunjača, J.; Kučić Grgić, D.; Voća, N. Prediction of the Production of Separated Municipal Solid Waste by Artificial Neural Networks in Croatia and the European Union. *Sustainability* **2022**, *14*, 10133. [[CrossRef](#)]
31. Rajković, D.; Marjanović Jeromela, A.; Pezo, L.; Lončar, B.; Zanetti, F.; Monti, A.; Kondić Špika, A. Yield and quality prediction of winter rapeseed—Artificial neural network and random forest models. *Agronomy* **2021**, *12*, 58. [[CrossRef](#)]
32. Dimić, I.; Pezo, L.; Rakić, D.; Teslić, N.; Zeković, Z.; Pavlić, B. Supercritical Fluid Extraction Kinetics of Cherry Seed Oil: Kinetics Modeling and ANN Optimization. *Foods* **2021**, *10*, 1513. [[CrossRef](#)]
33. Neto, J.G.; Ozorio, L.V.; de Abreu, T.C.C.; Dos Santos, B.F.; Pradelle, F. Modeling of biogas production from food, fruits and vegetables wastes using artificial neural network (ANN). *Fuel* **2021**, *285*, 119081. [[CrossRef](#)]
34. Yoon, Y.; Swales, G.; Margavio, T.M. Comparison of Discriminant Analysis versus Artificial Neural Networks. *J. Oper. Res. Soc.* **2017**, *44*, 51–60. [[CrossRef](#)]
35. Pestorić, M.; Sakač, M.; Pezo, L.; Škrobot, D.; Nedeljković, N.; Jovanov, P.; Filipčev, B.; Mandić, A. Physicochemical Changes of the Gluten-Free Rice-Buckwheat Cookies during Storage—Artificial Neural Network Model. *Period. Polytech. Chem. Eng.* **2019**, *63*, 609–617. [[CrossRef](#)]
36. Yang, Z.; Yang, Z.; Yu, F.; Tao, Z. Ultrasound-assisted heat pump intermittent drying of adzuki bean seeds: Drying characteristics and parameter optimization. *J. Food Process. Eng.* **2020**, *43*, e13501. [[CrossRef](#)]
37. Kaveh, M.; Taghinezhad, E.; Witrowa-Rajchert, D.; Imanian, K.; Khalife, E.; Nowacka, M. Use of ultrasound pre-treatment before microwave drying of kiwifruits—An optimization approach with response surface methodology. *J. Food Process. Preserv.* **2022**, *46*, e16714. [[CrossRef](#)]
38. Motevali, A.; Minaei, S.; Khoshtaghaza, M.H.; Amirnejat, H. Comparison of energy consumption and specific energy requirements of different methods for drying mushroom slices. *Energy* **2011**, *36*, 6433e6441. [[CrossRef](#)]

39. Yolmeh, M.; Jafari, S.M. Applications of response surface methodology in the food industry processes. *Food Bioprocess Technol.* **2017**, *10*, 413–433. [[CrossRef](#)]
40. Abdolrasol, M.G.; Hussain, S.S.; Ustun, T.S.; Sarker, M.R.; Hannan, M.A.; Mohamed, R.; Ali, J.A.; Mekhilef, S.; Milad, A. Artificial neural networks based optimization techniques: A review. *Electronics* **2021**, *10*, 2689. [[CrossRef](#)]
41. Atikler, U.; Demir, H.; Tokatlı, F.; Tihminlioğlu, F.; Balköse, D.; Ülkü, S. Optimisation of the effect of colemanite as a new synergistic agent in an intumescent system. *Polym. Degrad. Stab.* **2006**, *91*, 1563–1570. [[CrossRef](#)]
42. Granato, D.; Ares, G. *2014 Mathematical and Statistical Methods in Food Science and Technology*; John Wiley & Sons, Ltd. Print: Hoboken, NJ, USA, 2014; ISBN 9781118433683. [[CrossRef](#)]
43. Kat, C.J.; Els, P.S. Validation metric based on relative error. *Math. Comput. Model. Dyn. Syst.* **2012**, *18*, 487–520. [[CrossRef](#)]
44. Pezo, L.; Lončar, B.; Šovljanski, O.; Tomić, A.; Travičić, V.; Pezo, M.; Aćimović, M. Agricultural Parameters and Essential Oil Content Composition Prediction of Aniseed, Based on Growing Year, Locality and Fertilization Type—An Artificial Neural Network Approach. *Life* **2022**, *12*, 1722. [[CrossRef](#)] [[PubMed](#)]

**Disclaimer/Publisher’s Note:** The statements, opinions and data contained in all publications are solely those of the individual author(s) and contributor(s) and not of MDPI and/or the editor(s). MDPI and/or the editor(s) disclaim responsibility for any injury to people or property resulting from any ideas, methods, instructions or products referred to in the content.